

## H<sub>2</sub> Physisorbed on Graphane

C. Carbonell-Coronado · F. de Soto · C. Cazorla ·  
J. Boronat · M.C. Gordillo

Received: 6 July 2012 / Accepted: 2 November 2012 / Published online: 16 November 2012  
© Springer Science+Business Media New York 2012

**Abstract** We study the zero-temperature phase diagrams of H<sub>2</sub> adsorbed on the three structures predicted for graphane (chair, boat and washboard graphane), using a diffusion Monte Carlo technique. Graphane is the hydrogenated version of graphene, in which each carbon atom changes its hybridization to  $sp^3$  and forms a covalent bond with a hydrogen atom. Our results show that the ground state of H<sub>2</sub> adsorbed on all three types of graphane is a  $\sqrt{3} \times \sqrt{3}$  solid, similar to the structures found both for H<sub>2</sub> and D<sub>2</sub> on graphene. When the H<sub>2</sub> density increases, the system undergoes a first order phase transition to a triangular incommensurate solid. This change is direct in the case of washboard graphane, but indirect via different commensurate structures in the other cases. The total hydrogen weight percentage on the three graphane types in their ground states is in the range 10 % to 12 %, depending on if one or both graphane surfaces are covered with H<sub>2</sub>.

**Keywords** Graphane · Phase transitions · Molecular hydrogen

---

C. Carbonell-Coronado (✉) · F. de Soto · M.C. Gordillo  
Departamento de Sistemas Físicos, Químicos y Naturales, Universidad Pablo de Olavide de Sevilla,  
Ctra de Utrera km 1, 41013, Sevilla, Spain  
e-mail: [ccarbonell@upo.es](mailto:ccarbonell@upo.es)

C. Cazorla  
Institut de Ciència de Materials de Barcelona (ICMBA-CSIC), Campus UAB, 08193, Bellaterra,  
Spain

J. Boronat  
Departament de Física i Enginyeria Nuclear, Universitat Politècnica de Catalunya, B4-B5 Campus  
Nord, 08034 Barcelona, Spain

## 1 Introduction

The interest in graphene as a structure formally derived from graphite has risen lately, due, among other things, to the possibility of using it as adsorbent. Studying the physisorption of  $H_2$  on C-surfaces has the additional interest of assessing whether these surfaces could be used as reservoir in fuel cells. To do so, a certain amount of hydrogen has to be captured by the substrate. Hence, an ideal structure will be the hydrogenated version of graphene, which has been called graphane. In graphane, each carbon forms a covalent bond with a hydrogen atom. The existence of graphane was theoretically predicted by Sofo and collaborators [1], who proposed two different types of graphane, the chair graphane (C-graphane) and the boat one (B-graphane). Elias and collaborators [2] were able to synthesize the chair graphane in 2009. In 2010 a third type of graphane, the washboard graphane (W-graphane), was predicted [3].

Here, we present zero-temperature calculations of the phase diagrams of  $H_2$  adsorbed on the three different types of graphane, using the diffusion Monte Carlo technique. The aim of this work will be to compare those diagrams to those obtained on graphene and estimate the weight percentage of  $H_2$  that can be adsorbed on top of these novel structures.

The plan of this work is as follows. In Sect. 2 we will describe the computational method used in our calculations, indicating the parameters and auxiliary hypotheses necessary to carry out the simulations. In Sect. 3 the simulation results will be discussed and lastly, Sect. 4 will present our conclusions.

## 2 Method

In order to obtain the zero-temperature phase diagrams we have to solve the many-body Schrödinger equation for a set of  $H_2$  molecules adsorbed on graphane. The diffusion Monte Carlo method makes this possible for a system of bosons, such as the *para*- $H_2$  molecules considered here. The starting point of the method is the *trial function*, an initial approximation to the ground state wave function of the system. To simulate a liquid arrangement, we have to use the translational invariant. In this work, this means,

$$\Psi_L(\mathbf{r}_1, \mathbf{r}_2, \dots, \mathbf{r}_N) = \prod_{i < j} \exp\left[-\frac{1}{2}\left(\frac{b}{r_{ij}}\right)^5\right] \prod_i \Phi(\mathbf{r}_i), \quad (1)$$

where the first part is a Jastrow function that depends on the distances  $r_{ij}$  between each pair of  $H_2$  molecules, and the second one,  $\Phi(\mathbf{r}_i)$ , is the one-body wave function obtained by solving numerically the Schrödinger equation for a single  $H_2$  molecule in the potential created by all the carbon and hydrogen atoms on the graphane substrate.

On the other hand, to describe a solid phases, our trial was,

$$\Psi_S(\mathbf{r}_1, \mathbf{r}_2, \dots, \mathbf{r}_N) = \Psi_L \prod_{i,l=1}^N \exp\{-c[(x_i - x_l)^2 + (y_i - y_l)^2]\}, \quad (2)$$

i.e., we used the product of a liquid-like wave function by a Gaussian term whose purpose is to confine the H<sub>2</sub> molecules around the crystallographic positions ( $x_I, y_I$ ) corresponding to the particular solids we are interested in. The parameters  $b$  and  $c$  on Eq. (1) and Eq. (2) were optimized using previous Variational Monte Carlo calculations on each of the phases considered.

The H<sub>2</sub>–H<sub>2</sub> interactions were modeled by the Silvera and Goldman potential [4] and the H<sub>2</sub>–C and H<sub>2</sub>–H by a Lennard-Jone one. In this last case, we used the Lorentz-Berthelot combination rules to obtain the mixed parameters from the C–C and H–H interactions given in Ref. [5] and from the H<sub>2</sub>–H<sub>2</sub> ones in Ref. [6].

### 3 Results

A summary of our simulation results on C-graphane is displayed in Fig. 1. From there, we can see that the ground state for H<sub>2</sub> on this structure is a  $\sqrt{3} \times \sqrt{3}$  commensurate solid (solid circles in Fig. 1), since its energy per particle is lower than that of any other arrangement. This structure is similar to the ground state of H<sub>2</sub> on graphene [7]. When the H<sub>2</sub> density increases, we observe a phase transition (see Table 2) to a  $\delta$  commensurate phase (similar to the one obtained for D<sub>2</sub> on graphene [8, 9]) that changes to a triangular incommensurate solid (see Table 2) upon further hydrogen intake. The stability limits for these arrangements were determined by means of Maxwell double-tangent constructions. In this figure we also display the data for other structures: a 2/5 commensurate phase, a 3/7 commensurate arrangement and third structure found stable on B-graphane (see below). Any of those structures are metastable with respect to a mixture of the  $\sqrt{3} \times \sqrt{3}$  phase and the  $\delta$  phase (in the case of the 2/5 structure) or the incommensurate solid (for the 3/7 phase and the commensurate one), due to their relatively high energies per particle .

**Fig. 1** Energy per particle for different H<sub>2</sub> phases adsorbed on C-graphane. *Solid circle*,  $\sqrt{3} \times \sqrt{3}$  registered solid; *solid square*,  $\delta$  phase; *inverted solid triangles*, liquid arrangement; and *circles*, incommensurate triangular solid. *Solid triangle*, commensurate structure; *square*, 3/7 phase; *solid diamond*, 2/5 phase. The *dashed* and the *solid line* are fourth order polynomial fits to their corresponding data sets. The statistical error bars due to the uncertainties in the DMC calculation are smaller than the symbols are were not displayed for simplicity (Color figure online)

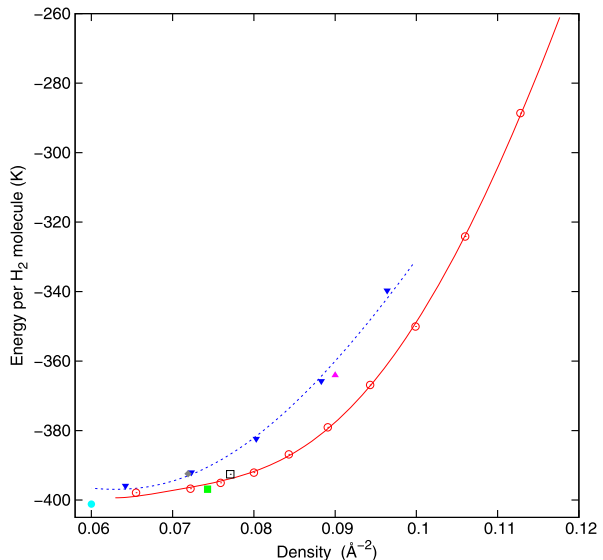


**Table 1** Energies per particle at the ground state ( $E_{\sqrt{3} \times \sqrt{3}}$ ), compared to the energies of the liquid phases at the same density ( $E_{liquid}$ ) for the three types of graphane. The result for the same structure on graphene is also shown for comparison [7]. In the solid structures, the error bars are the ones derived from the Diffusion Monte Carlo calculation, since these structures are produced at a single density. On the other hand, the uncertainties in the liquid densities derive from four order polynomial fits to obtain the minimum point in a energy versus density representation

	$E_{\sqrt{3} \times \sqrt{3}}/K$	$E_{liquid}/K$
C-graphane	$-401.180 \pm 0.005$	$-397 \pm 1$
B-graphane	$-407.09 \pm 0.01$	$-404.3 \pm 0.7$
W-graphane	$-414.140 \pm 0.005$	$-406.9 \pm 0.2$
Graphene [7]	$-461.12 \pm 0.01$	$-451.88 \pm 0.03^a$

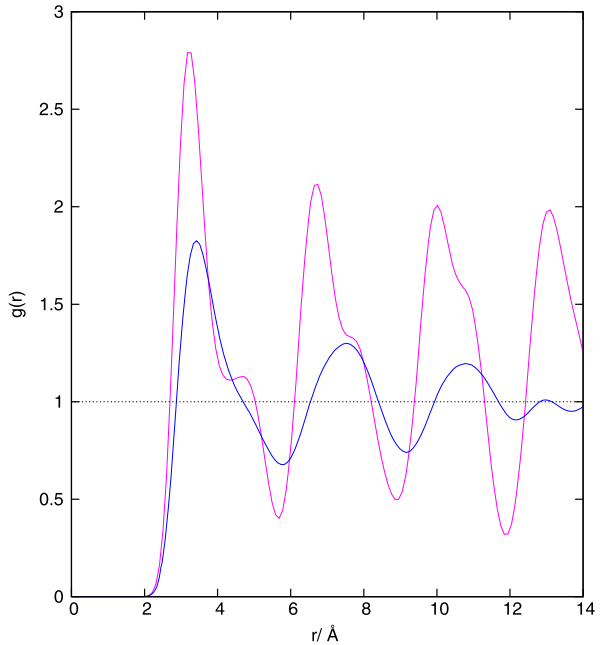
<sup>a</sup>Energy per H<sub>2</sub> molecule for the liquid phase at the equilibrium density  $\rho_0 = (0.05948 \pm 0.00005) \text{ \AA}^{-3}$

**Table 2** Stable phases and densities at which the phase transitions occur

	Phase	Density/ $\text{\AA}^{-2}$
C-graphane	$\sqrt{3} \times \sqrt{3}$	0.0600
	$\delta$	0.0743
	incommensurate	0.081
B-graphane	$\sqrt{3} \times \sqrt{3}$	0.0615
	$\delta$	0.0762
	commensurate	0.0922
	incommensurate	0.1032
W-graphane	$\sqrt{3} \times \sqrt{3}$	0.0674
	incommensurate	0.0719

In the case of H<sub>2</sub> adsorbed on B-graphane and W-graphane, our results also show that the lowest energy per particle in both cases corresponds to  $\sqrt{3} \times \sqrt{3}$  commensurate solid (see Table 1). In B-graphane (see Table 2), there is also a phase transition from a  $\sqrt{3} \times \sqrt{3}$  to a  $\delta$  phase, in a similar way to what happens on C-graphane. However, an increase in the hydrogen density does not produce a triangular incommensurate solid right away, but another stable commensurate structure. This is a novel arrangement, whose layout is displayed in Fig. 3. There, we show the projection of the positions on the  $z = 0$  plane of 300 H<sub>2</sub> configurations (each one containing a set of  $(x, y)$  coordinates taken from our simulations) on the B-graphane. Those projections produce the splotches displayed in Fig. 3, while the circles are the  $(x, y)$  coordinates of the C atoms of the graphane skeleton. The hydrogen atoms bound to those carbon atoms were not displayed for simplicity. We can see then that in this new structure, the H<sub>2</sub> molecules are located in between two of the carbon atoms whose C–H bonds point upwards. Since those positions are not isotropically distributed, the pair distribution function for this arrangement, displayed in Fig. 2, shows a set of two peaked maxima instead of the regular structures characteristic of a liquid phase.

**Fig. 2** Pair distribution functions on the  $xy$  plane for different structures on B-graphane. The *blue line* represents the liquid phase at a density of  $0.0740 \text{ \AA}^{-2}$  and the *purple one*, the new commensurate structure observed to be stable on B-graphane at a density of  $0.0921 \text{ \AA}^{-2}$  (Color figure online)



In the case of  $H_2$  adsorbed on W-graphane, the  $\delta$  phase is not stable. This means that the phase transition goes directly from a  $\sqrt{3} \times \sqrt{3}$  phase to a triangular incommensurate solid. In Fig. 4 we represent the pair distribution function for the stable triangular incommensurate phase at a density of  $0.0843 \text{ \AA}^{-2}$  and the corresponding ones for  $\delta$  and liquid phases at similar densities. From this figure, we can see that even the solid structures (the stable triangular phase and the unstable  $\delta$  solid) are more isotropic than the commensurate structure already described for the B-graphane. This is probably due to their smaller density in comparison to the one in the B-graphane. This increases the average distances between first (and successive) neighbors and blurs the differences between them to merge the maxima in the pair correlation functions.

### 4 Conclusions

We presented the zero-temperature  $H_2$  phase diagrams on three types of graphane. In all cases, the ground state is the  $\sqrt{3} \times \sqrt{3}$  commensurate solid, the similar result than the obtained for graphene [7]. From this structure, one or several phase transitions takes the system to a stable triangular incommensurate solid if the density increases enough. For W-graphane, the transition is direct. However, for C-graphane and B-graphane there are intermediate stable structures. In the case of C-graphane, the intermediate arrangement is a  $\delta$  phase, a commensurate solid similar to the found for  $D_2$  graphene and graphite [8]. On B-graphane, the phase transition goes first to the  $\delta$  commensurate phase and later to another commensurate structure.

**Fig. 3** Simulation cell used for the new commensurate solid on B-graphane. *Solid circles* are the projection of the positions of the carbon atoms on the  $z = 0$  plane. In *purple*, we represent the C atoms bound to the H atoms located on top of the carbon skeleton, while the *blue dots* are the C atoms bound to the H atoms located on the bottom part of the structure. The *rectangle* demarcates the unit cell of this arrangement (Color figure online)

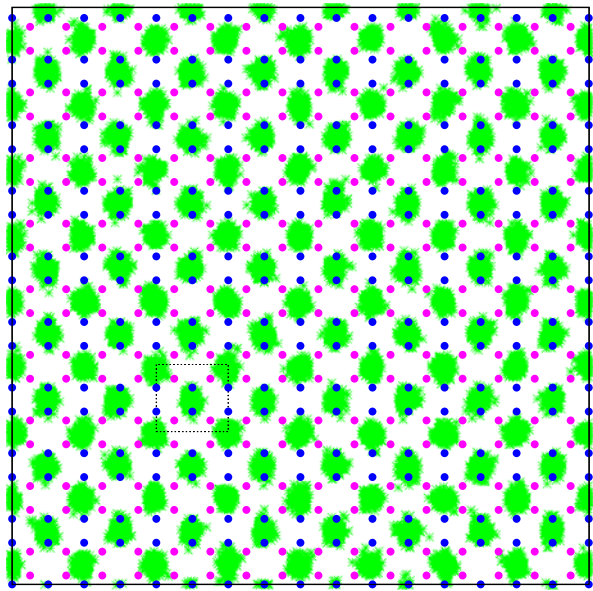
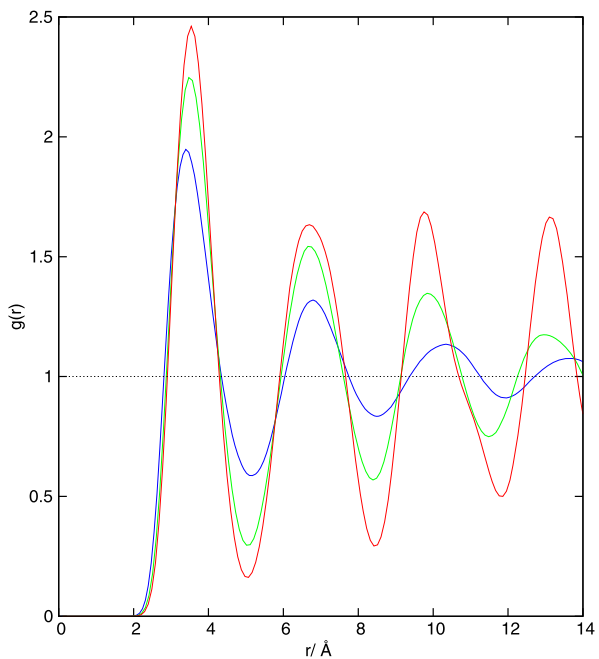


**Fig. 4** Pair distribution functions on the  $xy$  plane for different structures on W-graphane. The *blue line* represents the liquid phase at density  $0.0812 \text{ \AA}^{-2}$ , the *red* one the triangular incommensurate solid at density  $0.0843 \text{ \AA}^{-2}$  (stable phase) and the *green* one the delta phase at density  $0.0836 \text{ \AA}^{-2}$  (unstable arrangement) (Color figure online)



In graphane, each carbon is bound to a hydrogen atom. This means that in bare graphane the hydrogen weight percentage is 7.7 %. When  $\text{H}_2$  is added, the ground state (the one for which the total pressure is zero) is a  $\sqrt{3} \times \sqrt{3}$  phase, in which we have two  $\text{H}_2$  molecules on each unit cell containing three graphane hexagons. This

means that the total hydrogen percentage increases to about 10 % or 12 % depending on if one or both graphane surfaces are covered with H<sub>2</sub>. Those values are above the 6.5 % in weight necessary for graphane to be used in fuel cells. However, further tests would be necessary in order to ascertain if such a system is suitable for reversible H<sub>2</sub> adsorption in the working conditions of a fuel cell.

**Acknowledgements** We acknowledge partial financial support from the Junta de Andalucía Group PAI-205, Grant No. FQM-5985, MICINN (Spain) Grants No. FIS2010-18356 and FIS2011-25275, and Generalitat de Catalunya Grant 2009SGR-1003.

## References

1. J.O. Sofo, A.S. Chaudhari, G.D. Barber, *Phys. Rev. B* **75**, 153401 (2007)
2. D.C. Elias, R.R. Nair, T.M.G. Mohiuddin, S.V. Morozov, P. Blake, M.P. Halsall, A.C. Ferrari, D.W. Boukhvalov, M.I. Katsnelson, A.K. Geim, K.S. Novoselov, *Science* **323**, 610 (2009)
3. E. Cadelano, P.L. Palla, S. Giordano, L. Colombo, *Phys. Rev. B* **82**, 235414 (2010)
4. I.F. Silvera, V.V. Goldman, *J. Chem. Phys.* **69**, 4209 (1978)
5. J.M. Phillips, M.D. Hammerbacher, *Phys. Rev. B* **29**, 5859 (1984)
6. G. Stan, M.J. Bojan, S. Curtarolo, S.M. Gatica, M.W. Cole, *Phys. Rev. B* **62**, 2173 (2000)
7. M.C. Gordillo, J. Boronat, *Phys. Rev. B* **81**, 155435 (2010)
8. C. Carbonell-Coronado, M.C. Gordillo, *Phys. Rev. B* **85**, 155427 (2012)
9. H. Freimuth, H. Wiechert, H.P. Schildberg, H.J. Lauter, *Phys. Rev. B* **42**, 587 (1990)